

# Functionalized Ruthenium Dialkynyl Complexes with High Second-Order Nonlinear Optical Properties and Good Potential as Dye Sensitizers for Solar Cells

Filippo Nisic,<sup>†</sup> Alessia Colombo,<sup>\*,†</sup> Claudia Dragonetti,<sup>†,‡</sup> Eleonora Garoni,<sup>†</sup> Daniele Marinotto,<sup>‡</sup> Stefania Righetto,<sup>†</sup> Filippo De Angelis,<sup>\*,§</sup> Maria Grazia Lobello,<sup>§</sup> Paolo Salvatori,<sup>§</sup> Paolo Biagini,<sup>\*,||</sup> and Fabio Melchiorre<sup>||</sup>

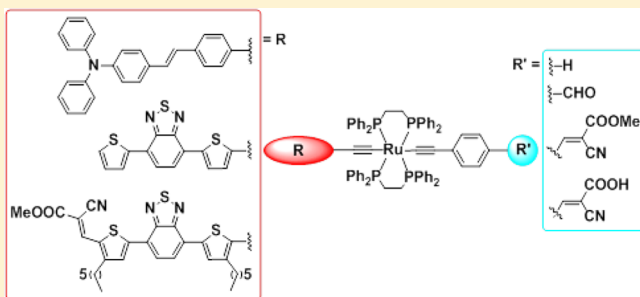
<sup>†</sup>Dipartimento di Chimica dell'Università degli Studi di Milano, UDR-INSTM, and <sup>‡</sup>ISTM-CNR, via Golgi 19, I-20133, Milano, Italy

<sup>§</sup>Computational Laboratory for Hybrid/Organic Photovoltaics (CLHYO), Istituto CNR di Scienze e Tecnologie Molecolari, Via Elce di Sotto 8, I-06213, Perugia, Italy

<sup>||</sup>Centro Ricerche per le Energie non Convenzionali, Istituto eni Donegani, via G. Fauser 4, 28100, Novara, Italy

## Supporting Information

**ABSTRACT:** Various dipolar  $\pi$ -delocalized Ru(II) dialkynyl complexes were prepared and characterized. Their second-order nonlinear optical (NLO) properties were investigated by the electric-field-induced second harmonic generation (EFISH) technique working in  $\text{CH}_2\text{Cl}_2$  solution with an incident wavelength of 1907 nm, whereas the dipole moments were determined by density functional theory (DFT) calculations. All the investigated complexes are characterized by a negative value of  $\mu\beta_{1,907 \text{ EFISH}}$  in agreement with a negative value of  $\Delta\mu_{\text{eg}}$  (difference of the dipole moment in the excited and ground state) upon excitation. Their second-order NLO response can be easily modulated by the nature of the alkynyl substituents. Besides, the most promising “push–pull” ruthenium diacetylide complex, adequately functionalized for anchoring to  $\text{TiO}_2$ , was tested as photosensitizer in dye-sensitized solar cells (DSSCs).



## INTRODUCTION

Compounds with second-order nonlinear optical (NLO) properties are of great interest as molecular building block materials for optical communications, optical data processing and storage, or electrooptical devices.<sup>1</sup> Among them, organometallic complexes represent a fascinating and growing class of second-order NLO chromophores that can offer additional flexibility, when compared to organic chromophores, due to the presence of metal–ligand charge-transfer transitions usually at relatively low energy and of high intensity, tunable by virtue of the nature, oxidation state, and coordination sphere of the metal center.<sup>1–6</sup>

In particular, metal  $\sigma$ -acetylides constitute a widely investigated class of second-order NLO chromophores, mainly developed by Humphrey et al.,<sup>7–9</sup> where the metal acts as the donor group of a Donor–Acceptor system connected by a  $\pi$ -linker. The almost linear  $\text{M}-\text{C}\equiv\text{C}-\text{R}$  structure allows a good coupling between the d metal orbitals and the  $\pi^*$  system of the  $\sigma$ -acetylide bridge, affording a significant NLO response controlled by low-energy MLCT excitations. Ruthenium  $\sigma$ -alkynyl complexes are very attractive, due to their facile high-yielding syntheses,<sup>10,11</sup> enhanced NLO coefficients,<sup>12,13</sup> easy construction of multimetallic dendrimers,<sup>14</sup> and reversible

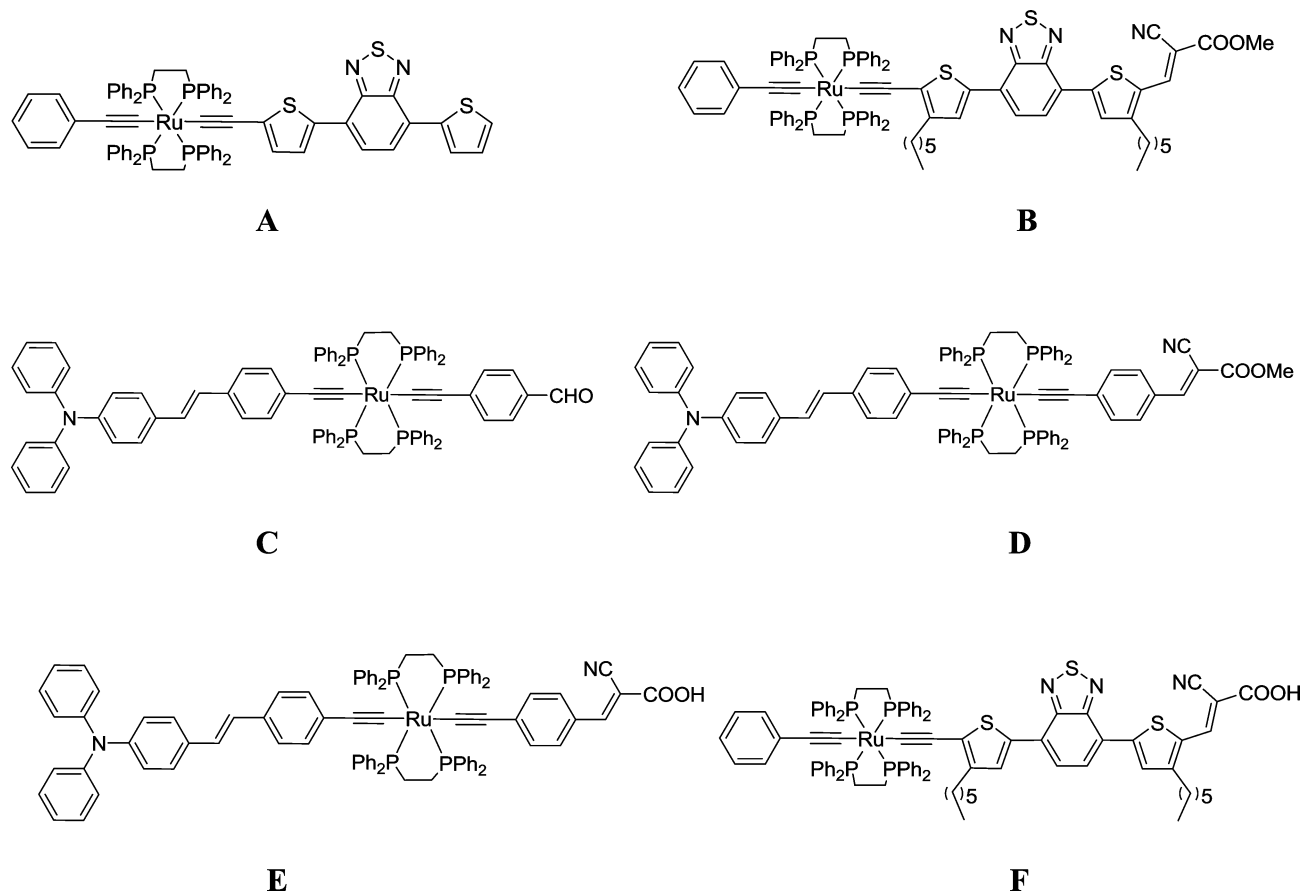
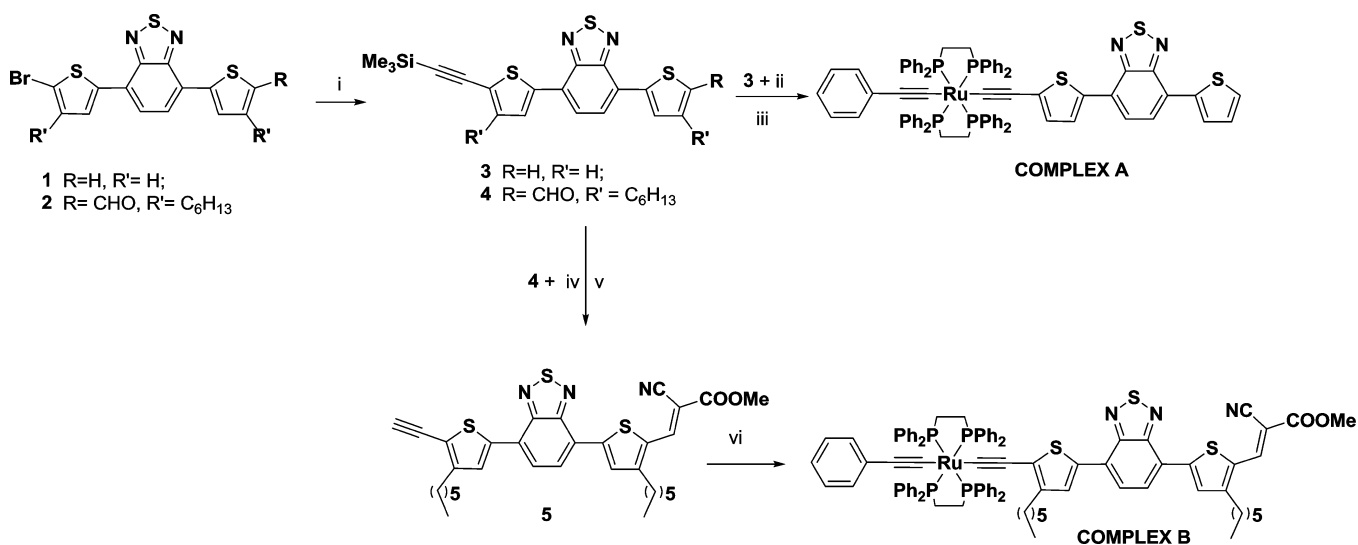
redox properties which afford the possibility of NLO switching.<sup>15</sup> Ruthenium  $\sigma$ -acetylides have been largely studied through hyper-Rayleigh (HRS) scattering measurements, but, to our knowledge, only in two cases through electric field second harmonic generation (EFISH) measurements.<sup>16,17</sup>

Thus, a few years ago, an EFISH study showed that dipolar alkynyl ruthenium complexes with a phenyleneethynylene or phenylenevinylene bridge between a donor “ClRu” moiety and a nitro acceptor group, such as *trans*-[Ru(4,4'-C $\equiv$ CC<sub>6</sub>H<sub>4</sub>C $\equiv$ CC<sub>6</sub>H<sub>4</sub>NO<sub>2</sub>)Cl(dppe)<sub>2</sub>] (dppe = Ph<sub>2</sub>PCH<sub>2</sub>CH<sub>2</sub>PPh<sub>2</sub>) and *trans*-[Ru{(E)-4,4',4''-C $\equiv$ CC<sub>6</sub>H<sub>4</sub>C $\equiv$ CC<sub>6</sub>H<sub>4</sub>CH=CHC<sub>6</sub>H<sub>4</sub>NO<sub>2</sub>}Cl(dppm)<sub>2</sub>] (dppm = Ph<sub>2</sub>PCH<sub>2</sub>PPh<sub>2</sub>), are characterized by good second-order NLO properties.<sup>16</sup> Also, very recently, some of us reported that a dinuclear Ru(II) complex, where two “phenylalkynyl-Ru” moieties are separated by a bridge consisting of 2,1,3-benzothiadiazole (BTD) flanked on either side by 2,5-thienyl units (Th), is characterized by an unexpected high EFISH NLO response where the benzothiadiazole moiety acts as an acceptor.<sup>17</sup> These observations prompted us to prepare novel dipolar mononuclear ruthenium

**Received:** September 11, 2014



Chart 1. Structure of the Investigated Ru(II) Complexes

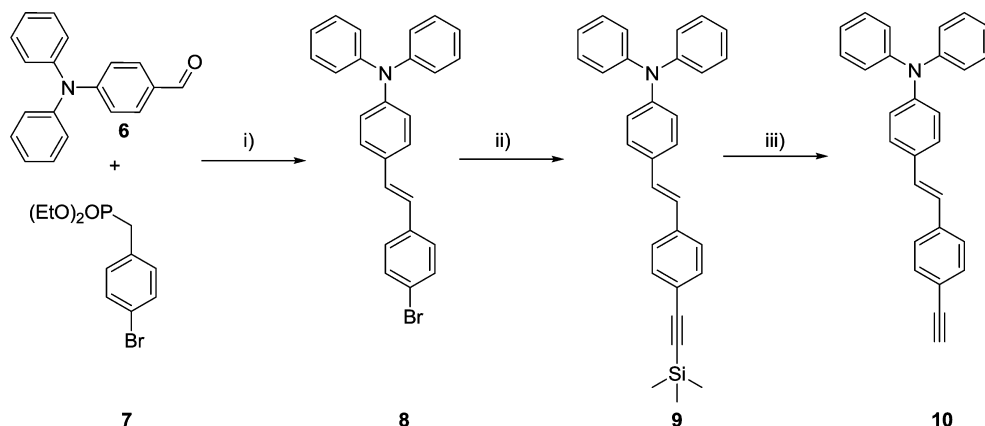
Scheme 1<sup>a</sup>

<sup>a</sup>(i) Trimethylsilylacetylene, Pd(PPh<sub>3</sub>)<sub>2</sub>Cl<sub>2</sub>, CuI, PPh<sub>3</sub>, TEA, 70 °C, 16 h, 80%; (ii) K<sub>2</sub>CO<sub>3</sub>, MeOH/THF, 24 h, 90%; (iii) *trans*-[ClRu(dppe)<sub>2</sub>C≡CPh], TEA, NaPF<sub>6</sub>, CH<sub>2</sub>Cl<sub>2</sub>, rt, 20 h, 85%; (iv) CNCH<sub>2</sub>COOMe, piperidine, MeOH, 50 °C, 3 h, 98%; (v) K<sub>2</sub>CO<sub>3</sub>, MeOH/THF, 40 °C, 3 h, 90%; (vi) *trans*-[ClRu(dppe)<sub>2</sub>C≡CPh], TEA, NaPF<sub>6</sub>, CH<sub>2</sub>Cl<sub>2</sub>, rt, 20 h, 70%.

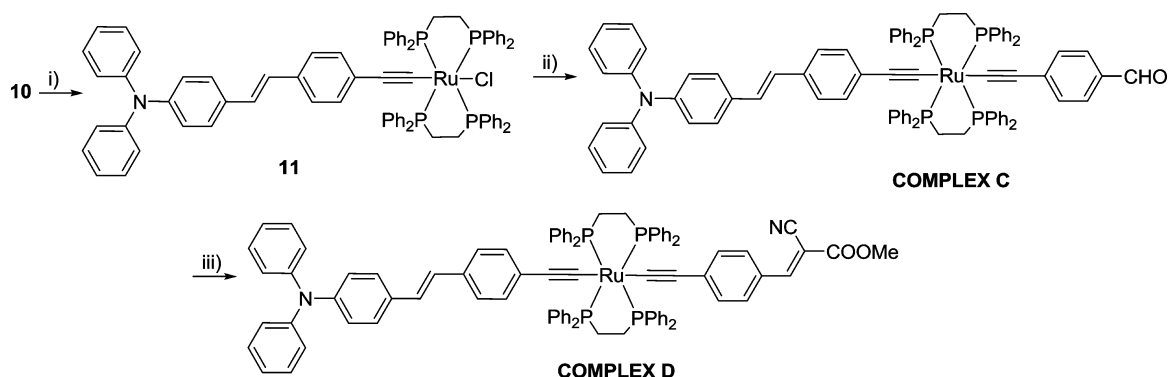
dialkynyl complexes (Chart 1) and to study their second-order NLO properties, using the EFISH technique, in order to get a better understanding of the 2,1,3-benzothiadiazole as acceptor moiety and to investigate new “Donor-phenylalkynyl-Ru-alkynylphenyl-Acceptor” architectures. The dipole moments

and the optical properties were evaluated by density functional theory (DFT) calculations.

But, thanks to the linear geometry of the alkynyl unit and its  $\pi$ -unsaturated character, metal alkynyls are attractive building blocks not only for the preparation of materials with optical nonlinearity but also for molecular wires and polymeric

Scheme 2<sup>a</sup>

<sup>a</sup>(i)  $t\text{BuO}^-\text{K}^+$ , THF, rt, 16 h, 80%; (ii) trimethylsilylacetylene,  $\text{Pd}(\text{PPh}_3)_2\text{Cl}_2$ , CuI,  $\text{PPh}_3$ , TEA, 70 °C, 16 h, 60%; (iii)  $\text{K}_2\text{CO}_3/\text{MeOH}$ , 24 h (95%).

Scheme 3<sup>a</sup>

<sup>a</sup>(i)  $\text{trans-}[\text{Ru}(\text{dppe})_2\text{Cl}_2]$ ,  $\text{NaPF}_6$ ,  $\text{CH}_2\text{Cl}_2$ , 40 °C 24 h, TEA, rt, 24 h 85%; (ii)  $p$ -ethynyl-benzaldehyde,  $\text{NaPF}_6$ , TEA,  $\text{CH}_2\text{Cl}_2$ , rt, 24 h 90%; (iii)  $\text{CNCH}_2\text{COOCH}_3$ , piperidine,  $\text{CH}_2\text{Cl}_2$ , rt, 18 h, 90%.

organometallic materials, which can possess interesting properties such as luminescence, liquid crystallinity, and electrical conductivity.<sup>18</sup> Metal–alkynyl complexes have been readily employed as simple electronic components with the ability to transport electronic charges between two points, allowing the study of intramolecular charge-transport mechanisms over long distances.<sup>19–21</sup> The ability of ruthenium to operate as a connector allowing electron flow to occur between different elements in *trans*-ditopic architectures was demonstrated,<sup>22–25</sup> and its exceptional propensity to serve as efficient electron relays in nanoscale oligomeric structures was reported.<sup>26–29</sup> Metal alkynyls also showed their potential as donor components of bulk heterojunction solar cells.<sup>30–34</sup>

We asked ourselves whether the *trans*-ruthenium diacetylide motif could act as an efficient relay within a “push–pull” architecture such as that of the new complex **D** and, therefore, could find application in the field of DSSCs. For this reason, we prepared the related complex **E** bearing a carboxylic acid anchoring group instead of the methyl ester function and studied in a preliminary way its potential as dye sensitizer for solar cells. For comparison, **F**, the carboxylic acid derivative of **B**, was also investigated.

## RESULTS AND DISCUSSION

**Synthesis.** Various novel ruthenium acetylide complexes (Chart 1) were prepared following the synthetic pathways shown in Schemes 1–3.

**A** and **B** were synthesized according to the simple synthetic strategy reported in Scheme 1: the starting materials *trans*- $\text{Ru}(\text{dppe})_2\text{Cl}_2$  and 4-(5-bromothiophen-2-yl)-7-(thiophen-2-yl)benzo[*c*][1,2,5]thiadiazole derivatives **1** and **2** were synthesized following reported methods.<sup>35</sup> **A** and **B** were obtained using an adaptation of the method of Humphrey et al.,<sup>36</sup> by reaction of the known  $[\text{ClRu}(\text{dppe})_2\text{C}\equiv\text{CPh}]$ <sup>37</sup> with the deprotected alkyne-derivative of **3** and with **5**. **F**, similar to **B** but with a carboxylic acid function instead of the methyl ester, was prepared starting from the potassium salt derivative of **5**; final acidification of the potassium salt of **B** with trifluoroacetic acid gave **F**.

In order to obtain **C** and **D**, we first prepare the acetylene derivative **10** as reported in Scheme 2; it was then reacted with *trans*- $[\text{Ru}(\text{dppe})_2\text{Cl}_2]$  as described in Scheme 3.

The 4-ethynyl-benzaldehyde was prepared according to the literature,<sup>38</sup> whereas (E)-4-(4-ethynylstyryl)-*N,N*-diphenyl-aniline **10** was synthesized as reported in Scheme 2. The *trans* isomer **8** was obtained by Horner–Hammonds reaction between 4-diphenyl-aminobenzaldehyde **6** and the phosphonate **7**.

The synthesis of the desired complexes **C** and **D** was accomplished by using terminal alkyne activation by ruthenium complexes,<sup>39</sup> thereby providing selective formation of vinylidene complexes that are the key intermediates for the formation of monoalkynyl complex **11** (by deprotonation with TEA) and unsymmetric bis-alkynyl complex **12** (by

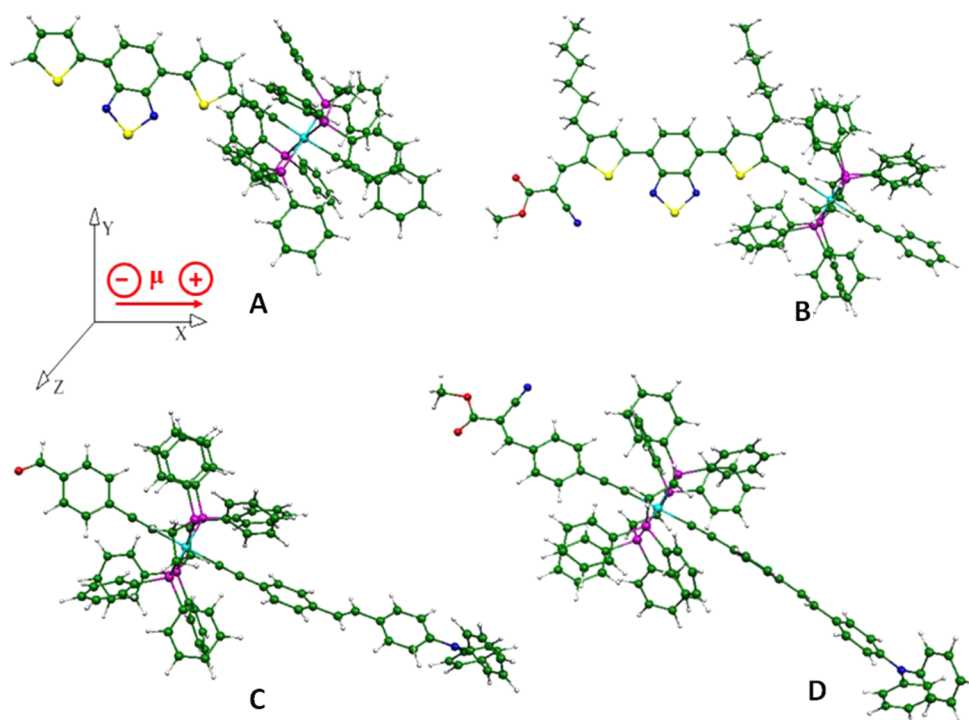


Figure 1. Optimized geometries of complexes A–D.

Table 1. Electronic Spectra,  $\mu\beta_{1.907 \text{ EFISH}}$ ,  $\mu$ , and  $\beta_{1.907 \text{ EFISH}}$  of the Investigated Ru(II) Complexes

complex	absorbance <sup>a</sup> $\lambda_{\text{max}}/\text{nm}$ [ $\epsilon/\text{M}^{-1} \text{ cm}^{-1}$ ]	$\mu\beta_{1.907 \text{ EFISH}}$ <sup>b</sup> ( $\times 10^{-48}$ ) esu	$\mu^c$ ( $\times 10^{-18}$ ) esu	$\beta_{1.907 \text{ EFISH}}^{d,g}$ ( $\times 10^{-30}$ ) esu
A	365 [36200], 489 [31400]	−1550	6.9	−225
B <sup>e</sup>	397 [28400], 497 [64400]	−1700	18.1	−94
C	289 [5600], 427 [9800]	−345	5.9	−58
D <sup>f</sup>	399 [21500], 437 [16300]	−780	7.9	−99

<sup>a</sup>In  $\text{CH}_2\text{Cl}_2$ . <sup>b</sup>Working in  $\text{CH}_2\text{Cl}_2$   $10^{-3}$  M with an incident radiation wavelength of  $1.907 \mu\text{m}$ ; the error is 10%. <sup>c</sup>Calculated at the B3LYP level in  $\text{CH}_2\text{Cl}_2$ ; in *vacuo*,  $\mu = 5.7, 13.54, 4.4$ , and  $6.0 \times 10^{-18}$  esu for complexes A, B, C, and D, respectively. At the CAM-B3LYP level,  $\mu$  values are slightly lower; see the Supporting Information. <sup>d</sup>By using  $\mu$  calculated in  $\text{CH}_2\text{Cl}_2$ ; by using  $\mu$  calculated in *vacuo*,  $\beta_{1.907 \text{ EFISH}} = -272, -126, -78$ , and  $-130 \times 10^{-30}$  esu for complexes A, B, C, and D, respectively. At the CAM-B3LYP level; see the Supporting Information. <sup>e</sup>For complex F:  $\lambda$  (nm) [ $\epsilon$  ( $\text{M}^{-1} \text{ cm}^{-1}$ )] = 395 [22500], 493 [59600]. <sup>f</sup>For complex E:  $\lambda$  (nm) [ $\epsilon$  ( $\text{M}^{-1} \text{ cm}^{-1}$ )] = 267 [17900], 428 [10700]. <sup>g</sup> $\beta_0$  values are reported in Table S12 in the Supporting Information.

introduction of a second alkynyl moiety at the ruthenium center of the monoalkynyl complex).

$[\text{RuCl}(\text{dppe})_2][\text{PF}_6]$  was generated from *trans*- $[\text{Ru}(\text{dppe})_2\text{Cl}_2]$  by chloride abstraction using sodium hexafluorophosphate and subsequently treated with the stoichiometric amount of (*E*)-4-(4-ethynylstyryl)-*N,N*-diphenylaniline **10** and TEA in order to form the monoalkynyl complex *trans*- $[\text{Ru}(\text{C}\equiv\text{C}-4-(\text{E})\text{-ethynylstyryl}-N,N\text{-diphenylaniline})\text{Cl}(\text{dppe})_2]$  **11**.

Using an analogous approach, the substitution of the remaining chloride ligand of **11** with 4-ethynylbenzaldehyde afforded **C**; subsequent condensation with methyl cyanoacetate in the presence of piperidine gave the target complex **D** in good yields. **E** was obtained in a similar manner by Knoevenagel condensation between **C** and cyanoacetic acid.

The molecular structures of the new compounds were characterized by using  $^1\text{H}$  NMR and mass spectroscopy.

**Optimized Geometry, Optical Properties, and Second-Order NLO Measurements.** In Figure 1, we report the optimized geometry in vacuum of A–D. Complex **A** is characterized by a quite planar arrangement of the donor-metal-acceptor backbone. The insertion of the hexyl chains on the thiophene moieties causes an increase of the dihedral angle

between the phenyl and the thiophene planes. Similarly to **B**, complexes **C**–**D** show a dihedral angle of about  $60^\circ$  between the donor and the acceptor groups.

The absorption maxima of the four complexes are reported in Table 1. TD-DFT calculations, by using two different exchange-correlation functionals, have been performed to gain information on the spectral features of the considered compounds. The B3LYP functional underestimates the  $\lambda_{\text{max}}$  in a range between 0.30 and 1.25 eV, for all the considered compounds. On the other hand, by considering a rigid shift of the excitation energies, a well-balanced description of the whole spectra, both in terms of energies and intensities, is obtained. The CAM-B3LYP functional better performs for complexes **A** and **B**, where a longer intramolecular charge transfer occurs, while, for **C** and **D**, the calculated excitation energies are overestimated by about 0.4 eV. A detailed list of the calculated excitation energies is reported in the Supporting Information. In all cases, the absorption band in the visible region is mainly characterized by HOMO (highest occupied molecular orbital)–LUMO (lowest unoccupied molecular orbital) transitions, with some contribution of the lower occupied molecular orbitals (HOMO-1/HOMO-2). The HOMOs of all the

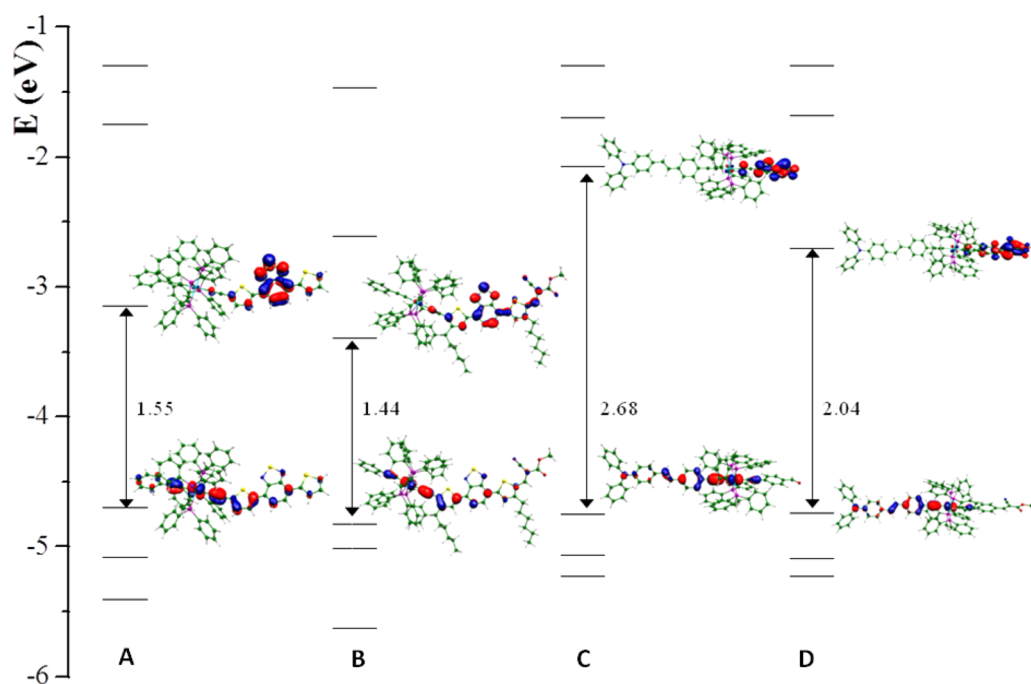


**Figure 2.** Schematic representation of the energy levels of complexes A–D. Isodensity surface plots (isodensity contour: 0.035) of HOMO and LUMO molecular orbitals are also shown.

investigated complexes are Ru orbitals combined with the  $\pi$  orbitals of thiophene and benzothiadiazole groups (complexes A–B) or of the (*E*)-4-(4-ethynylstyryl)-*N,N*-diphenylaniline (complexes C–D). The lowest unoccupied molecular orbitals (LUMOs) are instead completely localized on the acceptor moieties without any contribution from the metal (Figure 2). In particular, for complexes A–B, LUMO is strongly stabilized, due to the delocalization on the thiophene and benzothiadiazole groups. The presence of the methyl-cyanoacrylate moieties on the acceptor part of the complexes (complexes B–D) causes a further stabilization of the LUMO orbital.

In order to investigate their second-order NLO properties, the various ruthenium(II) complexes were investigated by the EFISH technique (see Table 1). It is known that this technique<sup>40–42</sup> can provide direct information on the intrinsic molecular NLO properties through eq 1

$$\gamma_{\text{EFISH}} = (\mu\beta_{\text{EFISH}}/5kT) + \gamma(-2\omega; \omega, \omega, 0) \quad (1)$$

where  $\mu\beta_{\text{EFISH}}/5kT$  is the dipolar orientational contribution and  $\gamma(-2\omega; \omega, \omega, 0)$ , a third-order term at frequency  $\omega$  of the incident light, is a purely electronic cubic contribution to  $\gamma_{\text{EFISH}}$  which can usually be neglected when studying the second-order NLO properties of dipolar compounds.<sup>5</sup>

In Table 1 are reported the  $\mu\beta_{1.907 \text{ EFISH}}$  values of all the investigated complexes, measured in  $\text{CH}_2\text{Cl}_2$  solution with an incident wavelength of 1.907  $\mu\text{m}$ . To obtain  $\beta_{1.907 \text{ EFISH}}$ , the projection along the dipole moment axis of the vectorial component of the tensor of the quadratic hyperpolarizability, it is necessary to know the dipole moment,  $\mu$ . In the present study, we used the theoretical dipole moments calculated as described in the Experimental Section (see also the Supporting Information).

All the novel investigated complexes are characterized by a negative value of  $\mu\beta_{1.907 \text{ EFISH}}$ , in agreement with a negative value of  $\Delta\mu_{\text{eg}}$  (difference of the dipole moment in the excited and ground state) upon excitation.<sup>5</sup> A negative  $\mu\beta_{1.907 \text{ EFISH}}$

value ( $-900 \times 10^{-48}$  esu) was also reported for the related dinuclear complex  $[\text{Ph-C}\equiv\text{C-Ru}(\text{dppe})_2\text{-C}\equiv\text{C-Th-BTD-Th-C}\equiv\text{C-Ru}(\text{dppe})_2\text{-C}\equiv\text{C-Ph}]$  (BTD = 2,1,3-benzothiadiazole; Th = 2,5-thienyl),<sup>17</sup> but A has a much higher absolute value of  $\mu\beta_{1.907 \text{ EFISH}}$  ( $-1550 \times 10^{-48}$  esu) due to a much higher dipole moment in the ground state ( $\mu$  of complex A is  $6.9 \times 10^{-18}$  esu, whereas  $\mu$  of  $[\text{Ph-C}\equiv\text{C-Ru}(\text{dppe})_2\text{-C}\equiv\text{C-Th-BTD-Th-C}\equiv\text{C-Ru}(\text{dppe})_2\text{-C}\equiv\text{C-Ph}]$ <sup>17</sup> is  $1.6 \times 10^{-18}$  esu). The value determined for B ( $-1700 \times 10^{-48}$  esu) is even higher due to a large increase of the dipole moment, attributed to the functionalization of the thienyl end-group with a methylcyanoacetate moiety, although the absolute value of  $\beta_{1.907 \text{ EFISH}}$  is lower (Table 1). The simple complex C with a “Donor-phenylalkynyl-Ru-alkynylphenyl-Acceptor” architecture (Donor =  $\text{Ph}_2\text{NPhCH=CH}$ ; Acceptor = CHO; see Chart 1) is characterized by the lowest  $\beta_{1.907 \text{ EFISH}}$  in agreement with the particularly high HOMO–LUMO gap (Figure 2),<sup>5</sup> which increases by a factor of 2.3 upon substitution of the aldehyde function by the more electron-withdrawing methylcyanoacetate moiety (D) due to an increase of both  $\mu$  and  $\beta_{1.907 \text{ EFISH}}$ . It is worth pointing out that the  $\mu\beta_{1.907 \text{ EFISH}}$  value of B is more than twice that of D, but this is due to a much higher dipole moment, the quadratic hyperpolarizability of both complexes being similar. Remarkably, A is characterized by the highest  $\beta_{1.907 \text{ EFISH}}$  value ( $-225 \times 10^{-30}$  esu) reported for a mononuclear alkynyl ruthenium complex,<sup>16</sup> in agreement with a quite planar arrangement of the donor-metal-acceptor backbone (Figure 1) and a low HOMO–LUMO gap (Figure 2). Calculation of the dipole moments with the CAM-B3LYP functional provides slightly lower values of  $\mu$ , and consequently higher  $\beta_{1.907 \text{ EFISH}}$  (see the Supporting Information). No significant differences were observed along the series of investigated complexes, making us confident about the employed computational setup.

**Complexes E and F in DSSCs.** Photoelectrochemical cells, capable of directly converting sunlight into electrical power, are



one of the most promising devices in the search for sustainable and renewable sources of clean energy. Dye-sensitized solar cells (DSSCs)<sup>43–52</sup> are considered a realistic solution for harnessing the energy of the sun and converting it into electrical energy, with power conversion efficiencies now exceeding the value of 12.3%.<sup>53</sup>

Solar light harvesting is the most important step of the photovoltaic process; consequently, the photosensitizer plays a key role in DSSCs. It might be characterized by an absorption spectrum that spans the entire visible range and extends into the near-IR region with a sufficiently high molar absorption coefficient. Moreover, the HOMO/LUMO energies of the dye must fit the conduction band of the photoanode semiconductor and the redox couple Nerst potential, in order to provide efficient charge transfer mechanisms. Ruthenium based coordination compounds bearing polypyridine ligands such as *cis*-di(thiocyanato)bis(2,2'-bipyridine-4,4'-dicarboxylate)Ru(II) (N3<sup>54,55</sup> and N719<sup>56,57</sup>) are among the most studied and performing photosensitizers. However, a serious drawback of such Ru(II) complexes is the presence of the anionic thiocyanate ligands which can be easily replaced, in working conditions, by other ligands which generally are contained, in high concentration, into the electrolyte solution, yielding a decrease of the efficiency during the lifetime of the device.<sup>58</sup> Therefore, a lot of efforts have been devoted to the preparation of thiocyanate-free ruthenium complexes for DSSCs.<sup>59–69</sup> Following our work on the use of diruthenium alkynyl complexes, as donor components of bulk heterojunction solar cells,<sup>34</sup> we anticipated that the *trans*-ruthenium diacetylide motif of **B** and **D** might act as an efficient relay within a “push–pull” architecture and, therefore, could find application in the field of DSSCs. For this reason, we prepared two new *trans*-diacetylide ruthenium compounds, **E** and **F**, both bearing the required cyano acrylic acid anchoring group, and we studied, in a preliminary way, their potentiality as dye sensitizers for solar cells.<sup>70</sup> The UV–vis spectra of **E** and **F** in dichloromethane solution show two main absorption bands at 267 nm ( $\epsilon = 17\,900\text{ M}^{-1}\text{ cm}^{-1}$ ), 428 nm ( $\epsilon = 10\,700\text{ M}^{-1}\text{ cm}^{-1}$ ) and 395 nm ( $\epsilon = 22\,500\text{ M}^{-1}\text{ cm}^{-1}$ ), 493 ( $\epsilon = 59\,600\text{ M}^{-1}\text{ cm}^{-1}$ ), respectively. It should be pointed out that the introduction of a carboxylic acid group produces a noticeable lowering of the  $\epsilon$  values and a slight blue shift of the absorption band (Table 1; compare **E** and **F** with **D** and **B**) with respect to those measured for the corresponding methyl ester derivatives, **D** and **B**.

Complex **F** shows a LUMO level of  $-3.43\text{ eV}$ , very similar to the methyl ester analogue, suggesting an unfavorable energy level alignment with the  $\text{TiO}_2$  conduction band edge for the electron injection. Similar LUMO values were found, at the same calculation level, for another class of sensitizers for which an inefficient electron injection process was highlighted as the main cause for the low photovoltaic performances.<sup>71</sup> On the other hand, the LUMO level of **E** ( $-2.78\text{ eV}$ ) appears to be adequate to allow the electron injection into  $\text{TiO}_2$  conduction band.

The main photovoltaic parameters of **E** and **F** are listed in Table 2, and they are compared, under the same experimental conditions, with those of the benchmark ruthenium dye N719.

As predicted from our theoretical calculations, **F** fails to act as a good dye sensitizer. The very low overall power conversion efficiency observed (0.3%, Table 2) could be ascribed to the incorrect matching of the energetic levels between the dye and  $\text{TiO}_2$  which practically impedes the passage of the electrons in the device. In fact, the low short-circuit photocurrent (1.5 mA/

**Table 2.** Main Photovoltaic Parameters<sup>a,b</sup> of DSSCs Based on Complexes **E** and **F**, in Comparison with Those Based on the Ruthenium Benchmark N719

dye	area/cm <sup>2</sup>	$J_{sc}/\text{mA cm}^{-2}$	$V_{oc}/\text{mV}$	FF	$\eta/\%$
<b>E</b>	0.0979	4.6	578	56.1	1.5
<b>F</b>	0.0898	1.5	432	46.5	0.3
<b>N719</b>	0.1025	15.2	745	71.9	8.1

<sup>a</sup>By using a black mask ( $0.1672\text{ cm}^2$ ). <sup>b</sup>Electrolyte composition: 0.6 M *N*-methyl-*N*-butylimidazolium iodide, 0.04 M iodine, 0.025 M LiI, 0.05 M guanidinium thiocyanate, 0.28 M *tert*-butylpyridine in 15/85 (v/v) mixture of valeronitrile/acetonitrile.

$\text{cm}^2$ ) and photovoltage levels are coherent with a poor charge transfer process.

A much better efficiency was obtained with **E** ( $\eta = 1.5\%$ ), although it does not reach a high value, as expected on the basis of its absorption spectrum (Table 1), which makes it capable to harvest only a little fraction of the sunlight. Moreover, the value measured in the IPCE curve (Figure 3), which does not exceed 20% in the visible region, suggests that, in this case, charge recombinations are very favorable processes and the attempt to mitigate them by employing 3 equiv of deoxycolic acid as coadsorbent does not lead to satisfactory results; in fact, the corresponding device shows, under the same conditions, an overall power conversion efficiency of 0.8%.

These results, together with those recently published by Tian and co-workers<sup>72–74</sup> on platinum diacetylide compounds and by Olivier et al.<sup>75</sup> on analogous ruthenium derivatives, show that it would be correct to propose D- $\pi$ -M- $\pi$ -A structured metal acetylide complexes as sensitizers for DSSCs with the aim to obtain the right compromise between the best efficiency together with a satisfactory stability. However, our results would indicate that, in such organometallic structures, the introduction of selected functional groups along the push–pull chain is a very subtle choice and seems to be crucial to obtain good efficiencies in DSSCs; in fact, by simple chemical changes in the donor moiety of the organometallic dye (introduction of a carbazole unit instead of a triphenylamine and removal of the styryl moiety), Olivier et al.<sup>75</sup> were able to overcome an overall power conversion efficiency of 7%, outperforming fully organic dyes of analogous structure. The main cause of the higher photovoltaic performance of their ruthenium sensitizer, compared to our complex **E**, can be highlighted in the better light harvesting ability ( $\lambda_{\text{max}}$  of 520 nm, with an  $\epsilon$  value of  $30\,200\text{ M}^{-1}\text{ cm}^{-1}$ ). This difference in the absorption spectrum is readily converted in a remarkable increase in the photocurrent value, reaching comparable levels with the standard N719 ruthenium dye.

## CONCLUSION

In summary, ruthenium(II) dialkynyl complexes are fascinating second-order NLO chromophores whose NLO response can be easily modulated by the nature of the alkynyl substituents, as confirmed by the electric-field-induced second harmonic generation technique. Remarkably, **A** and **B**, bearing a 2,1,3-benzothiadiazole flanked on either side by 2,5-thienyl units, are characterized by the largest values of  $\mu\beta_{1,907\text{ EFISH}}$  ever reported for alkynyl metal complexes and among the best reported for organometallic complexes.<sup>2–6</sup> They are excellent candidates for the preparation of second harmonic generation active polymeric films.<sup>76,77</sup> In addition,  $\pi$ -delocalized “push–pull” ruthenium diacetylide complexes, where a donor and an

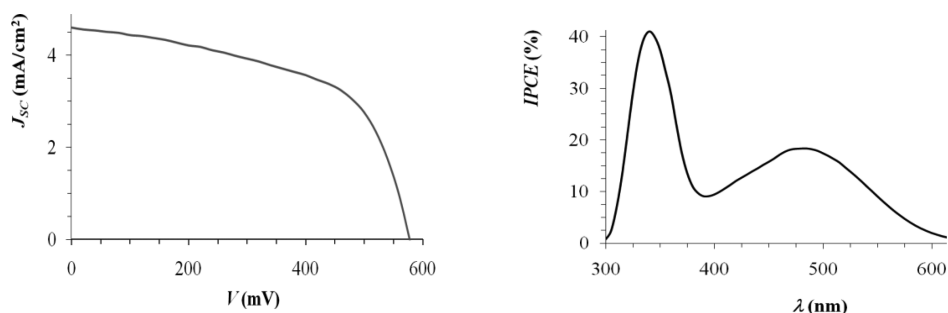


Figure 3. *JV* and IPCE curve for **E** measured in the conditions of Table 2.

acceptor units are separated by the metallic center, exhibit a promising application for the next generation of dye-sensitized solar cells.

## EXPERIMENTAL SECTION

**General Comments.** Solvents were dried by standard procedures: THF freshly distilled from Na/benzophenone under a nitrogen atmosphere; *N,N*-dimethylformamide (DMF) was dried over activated molecular sieves; toluene was distilled over Na/benzophenone, and triethylamine (Et<sub>3</sub>N) freshly distilled over KOH. All reagents were purchased from Sigma-Aldrich and were used without further purification. Reactions requiring anhydrous conditions were performed under nitrogen. <sup>1</sup>H and <sup>13</sup>C NMR spectra were recorded at 400 MHz on a Bruker AVANCE-400 instrument. Chemical shifts (δ) for <sup>1</sup>H and <sup>13</sup>C spectra are expressed in ppm relative to internal Me<sub>4</sub>Si as standard. Signals were abbreviated as s, singlet; bs, broad singlet; d, doublet; t, triplet; q, quartet; m, multiplet. Mass spectra were obtained with an FT-ICR Mass Spectrometer APEX II & Xmass software (Bruker Daltonics) - 4.7 Magnet and Autospec Fission Spectrometer (FAB ionization). MALDI-TOF mass spectra were obtained using a MICROFLEX-LT (BRUKER) with *trans*-2-[3-(4-*tert*-butylphenyl)-2-methyl-2-propenylidene] malononitrile (DCTB) as matrix. Samples for MALDI: 1 μL of complex solution + 49 μL of matrix solution + 0.5 μL of LiCl solution + 200 μL of CH<sub>2</sub>Cl<sub>2</sub>. The solutions were prepared as follows: 1 mg/mL in CH<sub>2</sub>Cl<sub>2</sub> for the complex, 10 mg of DCTB/mL for the matrix solution, and 10 mg of LiCl/mL in methanol for the salt solution.

Electronic absorption spectra were obtained using a Jasco V-530 spectrophotometer.

Thin-layer chromatography (TLC) was carried out with precoated Merck F<sub>254</sub> silica gel plates. Flash chromatography (FC) was carried out with Macherey-Nagel silica gel 60 (230–400 mesh).

**Synthesis of Complexes A and B (see Scheme 1 in Results and Discussion).** *Synthesis of Derivatives 3 and 4.* Under a nitrogen atmosphere, ethynyltrimethylsilane (33 μL, 0.23 mmol) was added to a degassed solution of the opportune bromo-derivative **1** or **2** (0.21 mmol), [PdCl<sub>2</sub>(PPh<sub>3</sub>)<sub>2</sub>] (4.0 mg, 0.02 mmol), CuI (2.0 mg, 0.04 mmol), and PPh<sub>3</sub> (2.0 mg, 0.02 mmol) in THF/triethylamine (12 mL, 1/2 v/v). The mixture was stirred for 20 h at 70 °C, and then the solvent was removed under reduced pressure. The residue was dissolved in dichloromethane and washed with water. The organic layer was dried over Na<sub>2</sub>SO<sub>4</sub>, and the solvent was removed at reduce pressure. The crude product was purified by flash chromatography on silica gel.

**3** was prepared starting from 4-(5-bromothiophen-2-yl)-7-(thiophen-2-yl)benzo[*c*][1,2,5]thiadiazole (79.4 mg). The crude product was purified using hexane/acetate 9:1 as eluent, affording the desired product as a red powder in 80% yield.

<sup>1</sup>H NMR (400 MHz, CDCl<sub>3</sub>, δ (ppm)) <sup>1</sup>H NMR (400 MHz, CDCl<sub>3</sub>, δ (ppm)) 8.15 (d, *J* = 3.8 Hz, 1H), 8.00 (d, *J* = 3.8 Hz, 1H), 7.88 (d, *J* = 7.6 Hz, 1H), 7.86 (d, *J* = 7.6 Hz, 1H), 7.49 (d, *J* = 4.8 Hz, 1H), 7.32 (d, *J* = 3.8 Hz, 1H), 7.23 (t, *J* = 4.6 Hz, 1H), 0.30 (s, 9H).

MS (FAB<sup>+</sup>) calcd for C<sub>19</sub>H<sub>16</sub>N<sub>2</sub>S<sub>3</sub>Si *m/z* 396.02, found 396. Anal. Calcd: C, 57.54; H, 4.07; N, 7.06. Found: C, 57.58; H, 4.06; N, 7.03.

**4** was prepared starting from the bromo derivative **2** (121.5 mg). The crude product was purified using hexane/acetate 8:2 as eluent, affording the product as a red powder in 78% yield.

<sup>1</sup>H NMR (400 MHz, CDCl<sub>3</sub>, δ (ppm)) <sup>1</sup>H NMR (400 MHz, CDCl<sub>3</sub>, δ (ppm)) 10.01 (s, 1H), 8.08 (s, 1H), 7.98 (d, *J* = 7.7 Hz, 1H), 7.95 (s, 1H), 7.87 (d, *J* = 7.7 Hz, 1H), 3.05 (t, *J* = 7.6 Hz, 2H), 2.78 (t, *J* = 7.6 Hz, 2H), 1.83–1.66 (m, 4H), 1.42–1.35 (m, 12H), 0.92–0.91 (m, 6H), 0.30 (s, 9H).

MS (FAB<sup>+</sup>) calcd for C<sub>32</sub>H<sub>40</sub>N<sub>2</sub>OS<sub>3</sub>Si *m/z* 592.21, found 592. Anal. Calcd: C, 64.82; H, 6.80; N, 4.72. Found: C, 64.89; H, 6.79; N, 4.73.

*Synthesis of Derivative 5.* To a solution of **4** (67.4 mg, 0.11 mmol) and methyl cyanoacetate (12 μL 0.125 mmol) in MeOH (5 mL) was added piperidine (13 μL, 0.55 mmol). After stirring at 50 °C for 3 h and overnight at room temperature, the solvent was removed under reduced pressure. The residue was purified by flash chromatography on silica gel (hexane/ethyl acetate 95:5). <sup>1</sup>H NMR (400 MHz, CDCl<sub>3</sub>, δ (ppm)) 8.50 (s, 1H), 8.22 (s, 1H), 8.03 (d, *J* = 7.8 Hz, 1H), 7.95 (s, 1H), 7.86 (d, *J* = 7.8 Hz, 1H), 2.93–2.91 (m, 2H), 2.80–2.76 (m, 2H), 1.74–1.55 (m, 6H), 1.35–1.27 (m, 10H), 0.94–0.91 (m, 6H), 0.30 (s, 9H).

50.0 mg (0.83 mmol) of alkyne was deprotected with K<sub>2</sub>CO<sub>3</sub> (126 mg, 0.91 mmol) in THF/MeOH (1:1) 6 mL at r.t for 1 h. The solvent was removed under reduced pressure, and the residue was purified by flash chromatography on silica gel (hexane/ethyl acetate 95:5). The product was obtained as a dark-red powder in 90% yield. <sup>1</sup>H NMR (400 MHz, CDCl<sub>3</sub>, δ (ppm)) 8.51 (s, 1H), 8.22 (s, 1H), 8.03 (d, *J* = 7.8 Hz, 1H), 7.96 (s, 1H), 7.84 (d, *J* = 7.8 Hz, 1H), 3.98 (s, 3H), 3.63 (s, 1H), 2.93–2.91 (m, 2H), 2.80–2.76 (m, 2H), 1.74–1.55 (m, 6H), 1.35–1.27 (m, 10H), 0.93–0.91 (m, 6H).

MS (FAB<sup>+</sup>) calcd for C<sub>33</sub>H<sub>35</sub>N<sub>3</sub>O<sub>2</sub>S<sub>3</sub> *m/z* 601.19, found 601. Anal. Calcd: C, 65.86; H, 5.86; N, 6.98. Found: C, 65.90; H, 5.87; N, 6.96.

*Synthesis of Complexes A and B: General Procedure.* A mixture of alkyne (0.07 mmol), *trans*-[Ru(dppe)<sub>2</sub>Cl<sub>2</sub>] (79.7 mg, 0.077 mmol), and NaPF<sub>6</sub> (26.9 mg, 0.16 mmol) in CH<sub>2</sub>Cl<sub>2</sub> (35 mL) was stirred in the dark for 18 h; triethylamine (45 μL) was added and stirring was maintained for 3h. The solvent was removed under reduced pressure, and the residue was taken up in CH<sub>2</sub>Cl<sub>2</sub> and purified by column chromatography on neutral alumina.

Complex **A** was prepared starting from the free alkyne 4-(5-ethynylthiophen-2-yl)-7-(thiophen-2-yl)benzo[*c*][1,2,5]thiadiazole (22.7 mg) obtained from **3** by deprotection with K<sub>2</sub>CO<sub>3</sub> in THF/MeOH as described in the synthesis of **5**.

<sup>1</sup>H NMR (400 MHz, CD<sub>2</sub>Cl<sub>2</sub>, δ (ppm)) 8.16 (m, 1H), 8.12 (d, *J* = 4.8 Hz, 1H), 8.08 (d, *J* = 5.4 Hz, 1H), 7.98 (d, *J* = 5.4 Hz, 1H), 7.88 (d, *J* = 4.8 Hz, 1H), 7.31–7.00 (m, 47H), 2.67 (m, 8H).

MS (MALDI-TOF, 2-[(2E)-3-(4-*tert*-butylphenyl)-2-methylprop-2-enylidene]malonitrile as the matrix) calcd for C<sub>76</sub>H<sub>60</sub>N<sub>2</sub>P<sub>4</sub>RuS<sub>3</sub> *m/z* 1322.19 found 1323. Anal. Calcd: C, 69.02; H, 4.57; N, 2.12. Found: C, 69.06; H, 4.55; N, 2.12.

Complex **B** was prepared starting from the free alkyne **5** (42.13 mg).

Elution with hexane/ethyl acetate 8:2 gave a purple band that was collected and dried in *vacuo*, affording the desired product in 75% yield.

$^1\text{H}$  NMR (400 MHz,  $\text{CD}_2\text{Cl}_2$ ,  $\delta$  (ppm)) 8.52 (s, 1H), 8.20 (s, 1H), 8.11 (d,  $J = 7.8$  Hz, 1H), 8.00 (s, 1H), 7.95 (d,  $J = 7.8$  Hz, 1H), 7.29–7.01 (m, 45H), 3.98 (s, 3H), 2.71 (m, 8H), 1.55–1.39 (m, 16H), 1.58–1.55 (m, 10H).

MS (MALDI-TOF, 2-[(2E)-3-(4-*tert*-butylphenyl)-2 methylprop-2-enylidene]malonitrile as the matrix) calcd for  $\text{C}_{93}\text{H}_{87}\text{N}_3\text{O}_2\text{P}_4\text{RuS}_3$   $m/z$  1599.40, found 1600.7. Anal. Calcd: C, 69.82; H, 5.48; N, 2.63. Found: C, 69.99; H, 5.39; N, 2.60.

Complex F was prepared starting from 45 mg of the potassium salt derivative of 5.

The intermediate was obtained in 95% yield in more basic condition than previous described for 5.

Starting from 4 (50 mg, 0.074 mmol),  $\text{K}_2\text{CO}_3$  (20.4 mg, 0.148 mmol) in THF/MeOH (1:1, 6 mL) at 30 °C for 1 h. The solvent was removed under reduced pressure, and the residue was purified by flash chromatography on silica gel (hexane/ethyl acetate 8:2). The acid was obtained dissolving the residue in  $\text{CH}_2\text{Cl}_2$  and adding the stoichiometric amount of trifluoroacetic acid.  $^1\text{H}$  NMR (400 MHz,  $\text{CD}_2\text{Cl}_2$ ,  $\delta$  (ppm)) 8.51 (s, 1H), 8.20 (s, 1H), 8.08 (d,  $J = 7.8$  Hz, 1H), 7.96 (s, 1H), 7.95 (d,  $J = 7.8$  Hz, 1H), 7.28–7.03 (m, 45H), 2.72 (m, 8H), 1.55–1.39 (m, 16H), 1.58–1.55 (m, 10H).

MS (MALDI-TOF, 2-[(2E)-3-(4-*tert*-butylphenyl)-2 methylprop-2-enylidene]malonitrile as the matrix) calcd for  $\text{C}_{92}\text{H}_{84}\text{KN}_3\text{O}_2\text{P}_4\text{RuS}_3$   $m/z$  1623.34, found 1624.0. Anal. Calcd: C, 68.04; H, 5.21; N, 2.59. Found: C, 68.02; H, 5.21; N, 2.60.

**Synthesis of Complexes C, D, and E (see Schemes 2 and 3 in Results and Discussion).** *Synthesis of (E)-4-(4-Bromostyryl)-N,N-diphenylaniline (8).* To a solution of diethyl 4-bromobenzylphosphonate (364.0 mg, 1.2 mmol, 1.1 equiv) and 4-(diphenylamino)benzaldehyde (295.0 mg, 1.08 mmol, 1 equiv) in THF (9 mL), under nitrogen, and cooled to 0 °C, was added, in small portions, potassium *tert*-butoxide (316.0 mg, 2.8 mmol, 2.6 equiv). The cool bath was then removed and the mixture stirred for 18 h at room temperature. After hydrolysis with water, the mixture was stirred for a further 30 min. The reaction mixture was diluted with AcOEt and washed with water: the organic layer was dried over  $\text{Na}_2\text{SO}_4$  and concentrated. The crude product obtained was purified by flash chromatography, using hexane/dichloromethane 1:1 as eluant, to give the product as a pale yellow solid (378 mg; yield 85%). Characterization was performed by  $^1\text{H}$  and  $^{13}\text{C}$  NMR, and it is consistent with published data.

*Synthesis of (E)-N,N-Diphenyl-4-(4-((trimethylsilyl)ethynyl)styryl)-aniline (9).* To a solution of (E)-4-(4-bromostyryl)-N,N-diphenylaniline (8) (280.0 mg, 0.47 mmol, 1 equiv) and ethynyltrimethylsilane (69.2 mg, 0.7 mmol, 1.5 equiv) in a degassed tetrahydrofuran (7.8 mL), under a flow of nitrogen, were added  $[\text{PdCl}_2(\text{PPh}_3)_2]$  (13.2 mg, 4 mol %), CuI (5.4 mg, 6 mol %), and triethylamine (2 mL). The reaction mixture was left under stirring at 70 °C overnight. The solvent was removed under reduced pressure, and the residue was purified by flash chromatography, using hexane/dichloromethane 9:1 as eluant, to give 9 as a yellow solid (157 mg; yield 75%). Characterization was performed by  $^1\text{H}$  and  $^{13}\text{C}$  NMR, and it is consistent with published data.

*Synthesis of (E)-4-(4-Ethynylstyryl)-N,N-diphenylaniline (10).* To a solution of (E)-N,N-diphenyl-4-(4-((trimethylsilyl)ethynyl)styryl)-aniline (9) (71.3 mg, 0.16 mmol, 1 equiv), in methanol (5.3 mL), under a flow of nitrogen, was added  $\text{K}_2\text{CO}_3$  anhydrous (88.4 mg, 0.64 mmol, 4 equiv). The reaction mixture was left under stirring at room temperature overnight. The solvent was removed under reduced pressure, and the residue was diluted with  $\text{CH}_2\text{Cl}_2$  and washed with water: the organic layer was dried over  $\text{Na}_2\text{SO}_4$  and concentrated. The crude product obtained was purified by flash chromatography, using hexane/dichloromethane 8:2 as eluant, to give 5 as a yellow solid (54.0 mg; yield 90%). MS(FAB $^+$ ):  $m/z$  371. Characterization was performed by  $^1\text{H}$  and  $^{13}\text{C}$  NMR, and it is consistent with published data.

*Synthesis of trans-[Ru(C $\equiv$ C-4-(E)-Ethynylstyryl)-N,N-diphenylaniline]Cl(dppe) $_2$ [PF $_6$ ] $_2$  (11).* trans-[Ru(dppe) $_2\text{Cl}_2$ ] (20.0 mg, 0.019 mmol) and NaPF $_6$  (3.6 mg, 0.0216 mmol) were dissolved in  $\text{CH}_2\text{Cl}_2$  (1 mL), and the solution was stirred for 12 h at room temperature with exclusion of light.

(E)-4-(4-ethynylstyryl)-N,N-diphenylaniline (8.0 mg, 0.0216 mmol) was added, and the solution was heated at 40 °C for 2 h. After cooling to room temperature, the reaction mixture was filtered, and the inorganic salts were washed with  $\text{CH}_2\text{Cl}_2$  (1 mL). Et $_2\text{O}$  was added to the  $\text{CH}_2\text{Cl}_2$  extract to precipitate the vinylidene salt as a violet powder, which was collected by filtration and then under nitrogen was redissolved in  $\text{CH}_2\text{Cl}_2$  (1 mL). TEA (50  $\mu\text{L}$ ) was added and stirring was maintained for 2 h, the solvent was removed under reduced pressure, and the residue was taken up in  $\text{CH}_2\text{Cl}_2$  and purified by column chromatography (basic alumina). Elution with  $\text{CH}_2\text{Cl}_2$  gave a yellow band that was collected and dried in *vacuo*. The yellow product was obtained in 85% yield.

$^1\text{H}$  NMR (400 MHz,  $\text{CD}_2\text{Cl}_2$ ): 7.77 (d,  $J_{\text{H-H}} = 8.6$  Hz, 2H), 7.40–7.19 (m, 20H), 7.13 (d,  $J_{\text{H-H}} = 8.6$  Hz, 2H), 7.11–6.98 (m, 36H), 2.68 (m, 8H). Elemental Analysis: Calcd for  $\text{C}_{80}\text{H}_{68}\text{ClNP}_4\text{Ru}$ : C, 73.70; H, 5.26; N, 1.07. Found: C, 74.05; H, 5.29; N, 1.09.

*Synthesis of Complex C. 11* (25.0 mg, 0.019 mmol), 4-ethynylbenzaldehyde (2.6 mg, 0.02 mmol), and NaPF $_6$  (1.0 mg, 0.076 mmol) were dissolved in  $\text{CH}_2\text{Cl}_2$  (2 mL), and the solution was stirred for 1 h. TEA (50  $\mu\text{L}$ ) was added, and stirring was maintained for 24 h at room temperature with exclusion of light. The reaction mixture was filtered, the inorganic salts were washed with  $\text{CH}_2\text{Cl}_2$  (1 mL), and the solvent was removed under reduced pressure.

The residue was taken up in  $\text{CH}_2\text{Cl}_2$  and purified by chromatography on neutral alumina, elution with hexane/ $\text{CH}_2\text{Cl}_2$  9:1, and then 1:1 gave an orange band that was collected and evaporated under reduced pressure. The orange product was obtained in 90% yield.

$^1\text{H}$  NMR (400 MHz,  $\text{CD}_2\text{Cl}_2$ ): 9.95 (s, 1H), 7.74 (d,  $J_{\text{H-H}} = 8.6$  Hz, 2H), 7.40–7.19 (m, 19H), 7.13 (d,  $J_{\text{H-H}} = 8.6$  Hz, 2H), 7.11–6.98 (m, 37H), 6.93 (d,  $J_{\text{H-H}} = 8.9$  Hz, 2H), 6.78 (d,  $J_{\text{H-H}} = 8.9$  Hz, 2H), 2.68 (m, 8H). Elemental Analysis: Calcd for  $\text{C}_{89}\text{H}_{73}\text{NOP}_4\text{Ru}$ : C, 76.49; H, 5.27; N, 1.00. Found: C, 76.89; H, 5.25; N, 0.98.

*Synthesis of Complexes D and E.* To a solution of Complex C (10.0 mg, 0.007 mmol) and methylcyanoacetate (2.52  $\mu\text{L}$ , 0.02 mmol) or cyanoacetic acid (13.0 mg, 0.02 mmol) in acetonitrile/ $\text{CH}_2\text{Cl}_2$  1:1 (4 mL) was added piperidine (10  $\mu\text{L}$ , 0.431 mmol, 7.0 equiv). After stirring at room temperature overnight, the solvent was removed under reduced pressure. The residue was taken up in  $\text{CH}_2\text{Cl}_2$  and diethyl ether was added, and the precipitate was filtered, and was washed with diethyl ether (1 mL). The filtrate was evaporated under reduced pressure, and the product was recrystallized.

Complex D: Orange/red product was obtained by slow diffusion of pentane into  $\text{CH}_2\text{Cl}_2$  solution (8.0 mg, 80%).  $^1\text{H}$  NMR (400 MHz,  $\text{CD}_2\text{Cl}_2$ ): 8.03 (s, 1H), 7.72 (d,  $J_{\text{H-H}} = 8.6$  Hz, 2H), 7.55–7.44 (m, 19H), 7.30 (d,  $J_{\text{H-H}} = 8.6$  Hz, 2H), 7.32–7.13 (m, 39H), 6.82–6.77 (m, 2H), 3.95 (s, 3H), 2.70 (m, 8H). Elemental Analysis: Calcd for  $\text{C}_{93}\text{H}_{76}\text{N}_2\text{O}_2\text{P}_4\text{Ru}$ : C, 75.55; H, 5.18; N, 1.89. Found: C, 75.59; H, 5.16; N, 1.89 MS(MALDI) calcd.  $m/z$ : 1478.34 found: 1478.0 (product), 897.2 (Ru(dppe) $_2$ ).

Complex E: The acid was obtained dissolving the residue in  $\text{CH}_2\text{Cl}_2$  and adding the stoichiometric amount of trifluoroacetic acid. Orange crystals of product were obtained by slow diffusion of pentane into  $\text{CH}_2\text{Cl}_2$  solution (9.0 mg, 91%).  $^1\text{H}$  NMR (400 MHz,  $\text{CD}_2\text{Cl}_2$ ): 8.05 (s, 1H), 7.78 (d,  $J_{\text{H-H}} = 8.6$  Hz, 2H), 7.60–7.44 (m, 19H), 7.35 (d,  $J_{\text{H-H}} = 8.6$  Hz, 2H), 7.32–7.13 (m, 39H), 6.82–6.77 (m, 2H), 2.70 (m, 8H). Elemental Analysis: Calcd for  $\text{C}_{92}\text{H}_{74}\text{N}_2\text{O}_2\text{P}_4\text{Ru}$ : C, 75.45; H, 5.09; N, 1.91. Found: C, 75.65; H, 5.07; N, 1.89 MS(MALDI)  $m/z$ : 1469.6 (COO $^-$ Li $^+$ ), 1270.3 (Ru(C $\equiv$ C-4-(E)-ethynylstyryl)-N,N-diphenylaniline) (dppe) $_2$ , 897.2 (Ru(dppe) $_2$ ).

**EFISH Measurements.** All EFISH measurements<sup>40–42</sup> were carried out at the Dipartimento di Chimica of the Università degli Studi di Milano, in  $\text{CH}_2\text{Cl}_2$  solutions at a concentration of  $1 \times 10^{-3}$  M, working with a nonresonant incident wavelength of 1.907  $\mu\text{m}$ , obtained by Raman-shifting the fundamental 1.064  $\mu\text{m}$  wavelength produced by a Q-switched, mode-locked Nd $^{3+}$ :YAG laser manufactured by Atalaser. The apparatus for the EFISH measurements is a prototype made by SOPRA (France). The  $\mu\beta_{\text{EFISH}}$  values reported are the mean values of 16 successive measurements performed on the



same sample. The sign of  $\mu\beta$  is determined by comparison with the reference solvent ( $\text{CH}_2\text{Cl}_2$ ).

**Computational Details.** All the calculations have been performed by the Gaussian 09 program package.<sup>78</sup> Geometry optimizations of the various ruthenium complexes were performed in *vacuo*, using the B3LYP exchange-correlation functional<sup>79</sup> and using a LANL2DZ basis set<sup>80</sup> for all atoms along with the corresponding pseudopotentials for Ru. On the optimized geometries, dipole moments have been calculated by single point, both in *vacuo* and in  $\text{CH}_2\text{Cl}_2$ , using the B3LYP functional and the LANL2DZ basis set (see the Supporting Information). Solvation effects were included by means of the conductor-like polarizable continuum model (C-PCM),<sup>81,82</sup> as implemented in G09. Then, the first 50 singlet excitations have been computed using TD-DFT at the same calculation level (B3LYP/LANL2DZ/C-PCM) on the optimized geometries. For comparative purposes, also the long-range corrected CAM-B3LYP functional was tested both in the dipole moments and in the excitation energies calculations.

**Fabrication and Evaluation of Solar Cells.**  $\text{TiO}_2$  electrodes were prepared by spreading (doctor blading) a colloidal  $\text{TiO}_2$  paste (20 nm sized; "Dyesol" DSL 18NR-T) onto a conducting glass slide (FTO, Hartford glass company, TEC 8, having a thickness of 2.3 mm and a sheet resistance in the range 6–9  $\Omega/\text{cm}^2$ ) that had been cleaned with water and EtOH treated with a plasma cleaner at 100 W for 10 min, dipped in a freshly prepared aqueous  $\text{TiCl}_4$  solution ( $4.5 \times 10^{-2}$  M), at 70 °C, for 30 min, and finally washed with ethanol. After a first drying at 125 °C for 15 min, a reflecting scattering layer containing >100 nm sized  $\text{TiO}_2$  ("Solaronix" Ti-Nanoxide R/SP) was bladed over the first  $\text{TiO}_2$  coat and sintered until 500 °C for 30 min. Then, the glass coated  $\text{TiO}_2$  was dipped again into a freshly prepared aqueous  $\text{TiCl}_4$  solution ( $4.5 \times 10^{-2}$  M), at 70 °C for 30 min, then washed with ethanol, and heated once more at 500 °C for 15 min. At the end of these operations, the final thickness of the  $\text{TiO}_2$  electrode was in the range 8–12  $\mu\text{m}$ , as determined by SEM analysis. After the second sintering, the FTO glass coated  $\text{TiO}_2$  was cooled at about 80 °C and immediately dipped into a  $\text{CH}_2\text{Cl}_2$  solution [ $1.5 \times 10^{-4}$  M] of the selected dye at r.t. for 18 h. The dyed titania glasses were washed with EtOH and dried at r.t. under a  $\text{N}_2$  flux. Finally, the excess of  $\text{TiO}_2$  was removed with a sharp Teflon penknife, and the exact active area of the dyed  $\text{TiO}_2$  was calculated by means of microphotography. A 50  $\mu\text{m}$  thick Surllyn spacer (TPS 065093-50 from Dyesol) was used to seal the photoanode and a platinized FTO counter electrode. Then, the cell was filled up with the desired electrolyte solution. The photovoltaic performance of the cells was measured with a solar simulator (Abet 2000) equipped with a 300 W xenon light source; the light intensity was adjusted with a standard calibrated Si solar cell ("VLSI Standard" SRC-1000-RTD-KG5). The current–voltage characteristics were acquired by applying an external voltage to the cell and measuring the generated photocurrent with a "Keithley 2602A" (3A DC, 10A Pulse) digital source meter.

## ■ ASSOCIATED CONTENT

### ● Supporting Information

Computational details and UV–vis spectra. This material is available free of charge via the Internet at <http://pubs.acs.org>.

## ■ AUTHOR INFORMATION

### Corresponding Authors

\*Tel: +39 0250314399. Fax: +39 0250314405. E-mail: [alessia.colombo@unimi.it](mailto:alessia.colombo@unimi.it) (A.C.).

\*Tel: +39 075 5855522. Fax: +39 075 585 5606. E-mail: [filippo@thch.unipg.it](mailto:filippo@thch.unipg.it) (F.D.A.).

\*Tel: +39 0321447817. Fax: +39 03217241. E-mail: [paolo.biagini@eni.com](mailto:paolo.biagini@eni.com) (P.B.).

### Notes

The authors declare no competing financial interest.

## ■ ACKNOWLEDGMENTS

We deeply thank Mattia Fontana for some experimental help. This work was supported by MIUR and by eni (Contract number 3500005452).

## ■ REFERENCES

- (1) Zyss, J. *Molecular Nonlinear Optics: Materials, Physics and Devices*; Academic Press: Boston, 1994.
- (2) Coe, B. J. *Acc. Chem. Res.* **2006**, 39, 383–393.
- (3) Cariati, E.; Pizzotti, M.; Roberto, D.; Tessore, F.; Ugo, R. *Coord. Chem. Rev.* **2006**, 250, 1210–1233.
- (4) Humphrey, M. G.; Samoc, M. *Adv. Organomet. Chem.* **2008**, 55, 61–136.
- (5) Di Bella, S.; Dragonetti, C.; Pizzotti, M.; Roberto, D.; Tessore, F.; Ugo, R. In *Molecular Organometallic Materials for Optics*; H., Le Bozec, Guerchais, V., Eds.; Topics in Organometallic Chemistry; Springer: Berlin, 2010; Vol. 28, pp 1–55.
- (6) Maury, O.; Le Bozec, H. In *Molecular Materials*; Bruce, D. W., O'Hare, D., Walton, R. I., Eds.; Wiley: Chichester, U.K., 2010; pp 1–59.
- (7) Powell, C. E.; Humphrey, M. G. *Coord. Chem. Rev.* **2004**, 248, 725–756.
- (8) Cifuentes, M. P.; Humphrey, M. G. *J. Organomet. Chem.* **2004**, 689, 3968–3981.
- (9) Guillaume, G.; Cifuentes, M. P.; Paul, F.; Humphrey, M. G. *J. Organomet. Chem.* **2014**, 751, 181–200.
- (10) McDonagh, A. M.; Whittall, I. R.; Humphrey, M. G.; Hockless, D. C. R.; Skelton, B. W.; White, A. H. *J. Organomet. Chem.* **1996**, 523, 33–40.
- (11) McDonagh, A. M.; Cifuentes, M. P.; Whittall, I. R.; Humphrey, M. G.; Samoc, M.; Luther-Davies, B.; Hockless, D. C. R. *J. Organomet. Chem.* **1996**, 526, 99–103.
- (12) Naulty, R. H.; McDonagh, A. M.; Whittall, I. R.; Cifuentes, M. P.; Humphrey, M. G.; Houbrechts, S.; Maes, J.; Persoons, A.; Heath, G. A.; Hockless, D. C. R. *J. Organomet. Chem.* **1998**, 563, 137–146.
- (13) Hurst, S. K.; Humphrey, M. G.; Morrall, J. P.; Cifuentes, M. P.; Samoc, M.; Luther-Davies, B.; Heath, G. A.; Willis, A. C. *J. Organomet. Chem.* **2003**, 670, 56–65.
- (14) Green, K. A.; Cifuentes, M. P.; Samoc, M.; Humphrey, M. G. *Coord. Chem. Rev.* **2011**, 255, 2025–2038.
- (15) Green, K. A.; Cifuentes, M. P.; Samoc, M.; Humphrey, M. G. *Coord. Chem. Rev.* **2011**, 255, 2530–2541.
- (16) Rigamonti, L.; Babgi, B.; Cifuentes, M. P.; Roberts, R. L.; Petrie, S.; Stranger, R.; Righetto, S.; Teshome, A.; Asselberghs, I.; Clays, K.; Humphrey, M. G. *Inorg. Chem.* **2009**, 48, 3562–3572.
- (17) Colombo, A.; Nisic, F.; Dragonetti, C.; Marinotto, D.; Oliveri, I. P.; Righetto, S.; Lobello, M. G.; De Angelis, F. *Chem. Commun.* **2014**, 50, 7986–7989.
- (18) Long, N. J.; Williams, C. K. *Angew. Chem., Int. Ed.* **2003**, 42, 2586–2617.
- (19) Owen, G. R.; Stahl, J.; Hampel, F. J.; Gladysz, A. *Chem.—Eur. J.* **2008**, 14, 73–87.
- (20) Ghazala, S. I.; Paul, F.; Toupet, L.; Roisnel, T.; Hapiot, P.; Lapinte, C. *J. Am. Chem. Soc.* **2006**, 128, 2463–2476.
- (21) Rigaut, S.; Olivier, C.; Costuas, K.; Choua, S.; Fadhel, O.; Massue, J.; Turek, P.; Saillard, J. Y.; Dixneuf, P. H.; Touchard, D. *J. Am. Chem. Soc.* **2006**, 128, 5859–5876.
- (22) Vacher, A.; Barrière, F.; Roisnel, T.; Piekara-Sady, L.; Lorcy, D. *Organometallics* **2011**, 30, 3570–3578.
- (23) Bruce, M. I.; Le Guennic, B.; Scoleri, N.; Zaitseva, N. N.; Halet, J.-F. *Organometallics* **2012**, 31, 4701–4706.
- (24) Wuttke, E.; Pevny, F.; Hervault, Y.-M.; Norel, L.; Drescher, M.; Winter, R. F.; Rigaut, S. *Inorg. Chem.* **2012**, 51, 1902–1915.
- (25) Marques-Gonzalez, S.; Yufit, D. S.; Howard, A. K.; Martin, S.; Osorio, H. M.; Garcia-Suarez, V. M.; Nichols, R. J.; Higgins, S. J.; Cea, P.; Low, P. J. *Dalton Trans.* **2013**, 42, 338–341.

- (26) Kim, B.; Beebe, J. M.; Olivier, C.; Rigaut, S.; Touchard, D.; Kushmerick, J. G.; Zhu, X. Y.; Frisbie, C. D. *J. Phys. Chem. C* **2007**, *111*, 7521–7526.
- (27) Olivier, C.; Choua, S.; Turek, P.; Touchard, D.; Rigaut, S. *Chem. Commun.* **2007**, 3100–3102.
- (28) Olivier, C.; Costuas, K.; Choua, S.; Maurel, V.; Turek, P.; Saillard, J.-Y.; Touchard, D.; Rigaut, S. *J. Am. Chem. Soc.* **2010**, *132*, 5638–5651.
- (29) Luo, L.; Benameur, A.; Brignou, P.; Choi, S. H.; Rigaut, S.; Frisbie, C. D. *J. Phys. Chem. C* **2011**, *115*, 19955–19961.
- (30) Wong, W.-Y.; Ho, C.-L. *Acc. Chem. Res.* **2010**, *43*, 1246–1256 and references therein.
- (31) Wong, W.-Y.; Wang, X.-Z.; He, Z.; Djuricic, A. B.; Yip, C.-T.; Cheung, K.-Y.; Wang, H.; Mak, C. S. K.; Chan, W.-K. *Nat. Mater.* **2007**, *6*, 521–527.
- (32) Baek, N. S.; Hau, S. K.; Yip, H.-L.; Acton, O.; Chen, K.-S.; Jen, A. K.-Y. *Chem. Mater.* **2008**, *20*, 5734–5736.
- (33) Mei, J.; Ogawa, K.; Kim, Y.-G.; Heston, N. C.; Arenas, D. J.; Nasrollahi, Z.; McCarley, T. D.; Tanner, D. B.; Reynolds, J. R.; Schanze, K. S. *ACS Appl. Mater. Interfaces* **2009**, *1*, 150–161.
- (34) Colombo, A.; Dragonetti, C.; Roberto, D.; Ugo, R.; Falciola, L.; Luzzati, S.; Kotowski, D. *Organometallics* **2011**, *30*, 1279–1282.
- (35) Dai, F.-R.; Zhan, H.-M.; Liu, Q.; Fu, Y.-Y.; Li, J.-H.; Wang, Q.-W.; Xie, Z.; Wang, L.; Yan, F.; Wong, W.-Y. *Chem.—Eur. J.* **2012**, *18*, 1502–1511.
- (36) Grelaud, G.; Cifuentes, M. P.; Schwich, T.; Argouarch, G.; Petrie, S.; Stranger, R.; Paul, F.; Humphrey, M. G. *Eur. J. Inorg. Chem.* **2012**, 65–75.
- (37) Touchard, D.; Haquette, P.; Guesmi, S.; Le Pichon, L.; Daridor, A.; Toupet, L.; Dixneuf, P. H. *Organometallics* **1997**, *16*, 3640–3648.
- (38) Thorand, S.; Krause, N. *J. Org. Chem.* **1998**, *63*, 8551–8553.
- (39) Touchard, D.; Haquette, P.; Pirio, N.; Toupet, L.; Dixneuf, P. H. *Organometallics* **1993**, *12*, 3132–3139.
- (40) Levine, B. F.; Bethea, C. G. *Appl. Phys. Lett.* **1974**, *24*, 445–447.
- (41) Levine, B. F.; Bethea, C. G. *J. Chem. Phys.* **1975**, *63*, 2666–2682.
- (42) Ledoux, I.; Zyss, J. *Chem. Phys.* **1982**, *73*, 203–213.
- (43) Nazeeruddin, M. K.; Klein, C.; Liska, P.; Graetzel, M. *Coord. Chem. Rev.* **2005**, *249*, 1460–1467.
- (44) Bredas, J.-L.; Durrant, J. R. *Acc. Chem. Res.* **2009**, *42*, 1689–1690.
- (45) Graetzel, M. *Acc. Chem. Res.* **2009**, *42*, 1788–1798.
- (46) Nozik, A. J.; Miller, J. *Chem. Rev.* **2010**, *110*, 6443–6445.
- (47) Hagfeldt, A.; Boschloo, G.; Sun, L.; Kloo, L.; Pettersson, H. *Chem. Rev.* **2010**, *110*, 6595–6663.
- (48) Snaith, H. J. *Adv. Funct. Mater.* **2010**, *20*, 13–19.
- (49) Caramori, S.; Di Carlo, A.; Cristino, V.; Boaretto, R.; Argazzi, R.; Bignozzi, C. A. *Int. J. Photoenergy* **2010**, 1–16.
- (50) Caramori, S.; Bignozzi, C. A. Recent Developments in the Design of Dye Sensitized Solar Cell Components. In *Electrochemistry of Functional Supramolecular Systems*; J. Wiley & Sons: Hoboken, NJ, 2010; pp 523–579.
- (51) Spokoiny, A. M.; Li, T. C.; Farha, O. K.; Machan, C. W.; She, C.; Stern, C. L.; Marks, T. J.; Hupp, J. T.; Mirkin, C. A. *Angew. Chem., Int. Ed.* **2010**, *49*, 5339–5343.
- (52) Nazeeruddin, M. K.; Baranoff, E.; Grätzel, M. *Sol. Energy* **2011**, *85*, 1172–1178.
- (53) Yella, A.; Lee, H.-W.; Tsao, H. N.; Yi, C.; Chandiran, A. K.; Nazeeruddin, M. K.; Diau, E.W.-G.; Yeh, C.-Y.; Zakeeruddin, S. M.; Graetzel, M. *Science* **2011**, *334*, 629–634.
- (54) Nazeeruddin, M. K.; Kay, A.; Rodicio, I.; Humphry-Baker, R.; Mueller, E.; Liska, P.; Vlachopoulos, N.; Graetzel, M. *J. Am. Chem. Soc.* **1993**, *115*, 6382–6390.
- (55) Grätzel, M. *J. Photochem. Photobiol., A* **2004**, *164*, 3–14.
- (56) Nazeeruddin, M. K.; Splivallo, R.; Liska, P.; Comte, P.; Grätzel, M. *Chem. Commun.* **2003**, 1456–1457.
- (57) Nazeeruddin, M. K.; De Angelis, F.; Fantacci, S.; Selloni, A.; Viscardi, G.; Liska, P.; Ito, S.; Takeru, B.; Graetzel, M. *J. Am. Chem. Soc.* **2005**, *127*, 16835–16847.
- (58) Colombo, A.; Dragonetti, C.; Valore, A.; Coluccini, C.; Manfredi, N.; Abboto, A. *Polyhedron* **2014**, *82*, S0–S6.
- (59) Bessho, T.; Yoneda, E.; Yum, J. H.; Guglielmi, M.; Tavernelli, I.; Imai, H.; Rothlisberger, U.; Nazeeruddin, M. K.; Graetzel, M. *J. Am. Chem. Soc.* **2009**, *131*, 5930–5934.
- (60) Bomben, P. G.; Robson, K. C. D.; Sedach, P. A.; Berlinguette, C. P. *Inorg. Chem.* **2009**, *48*, 9631–9643.
- (61) Bomben, P. G.; Koivisto, B. D.; Berlinguette, C. P. *Inorg. Chem.* **2010**, *49*, 4960–4971.
- (62) Bomben, P. G.; Gordon, T. J.; Schott, E.; Berlinguette, C. P. *Angew. Chem., Int. Ed.* **2011**, *50*, 10682–10685.
- (63) Robson, K. C. D.; Sporinova, B.; Koivisto, B. D.; Baumgartner, T.; Yella, A.; Nazeeruddin, M. K.; Graetzel, M.; Berlinguette, C. P. *Inorg. Chem.* **2011**, *50*, 5494–5508.
- (64) Dragonetti, C.; Valore, A.; Colombo, A.; Roberto, D.; Trifiletti, V.; Manfredi, N.; Salamone, M. M.; Ruffo, R.; Abboto, A. *J. Organomet. Chem.* **2012**, *714*, 88–93.
- (65) Abboto, A.; Dell’Orto, E.; Coluccini, C.; Manfredi, N.; Trifiletti, V.; Salamone, M. M.; Ruffo, R.; Acciarri, M.; Colombo, A.; Dragonetti, C.; Ordanini, S.; Roberto, D.; Valore, A. *Dalton Trans.* **2012**, *41*, 11731–11738.
- (66) Abboto, A.; Manfredi, N.; Coluccini, C.; Roberto, D.; Ugo, R.; Dragonetti, C.; Valore, A.; Colombo, A. PCT Int. Appl. WO 2012013719 A1 20120202, 2012.
- (67) Dragonetti, C.; Colombo, A.; Magni, M.; Mussini, P.; Nisic, F.; Roberto, D.; Ugo, R.; Valore, A.; Valsecchi, A.; Salvatori, P.; Lobello, M. G.; De Angelis, F. *Inorg. Chem.* **2013**, *52*, 10723–10725.
- (68) Dragonetti, C.; Valore, A.; Colombo, A.; Magni, M.; Mussini, P.; Roberto, D.; Ugo, R.; Valsecchi, A.; Trifiletti, V.; Manfredi, N.; Abboto, A. *Inorg. Chim. Acta* **2013**, *405*, 98–104.
- (69) Wang, S.-W.; Wu, K.-L.; Ghadiri, E.; Lobello, M. G.; Ho, S.-T.; Chi, Y.; Moser, J.-E.; De Angelis, F.; Graetzel, M.; Nazeeruddin, M. K. *Chem. Sci.* **2013**, *4*, 2423–2433.
- (70) Contract with eni: number 3500005452; July 2010–June 2013.
- (71) Salvatori, P.; Amat, A.; Pastore, M.; Vitillaro, G.; Sudhakar, K.; Giribabu, L.; Soujanya, Y.; De Angelis, F. *Comput. Theor. Chem.* **2014**, *1030*, 59–66.
- (72) Wu, W.; Xu, X.; Yang, H.; Hua, J.; Zhang, X.; Zhang, L.; Long, Y.; Tian, H. *J. Mater. Chem.* **2011**, *21*, 10666–10671.
- (73) Dai, F.-R.; Chen, Y.-C.; Lai, L.-F.; Wu, W.-J.; Cui, C.-H.; Tan, G.-P.; Wang, X.-Z.; Lin, J.-T.; Tian, H.; Wong, W.-Y. *Chem.—Asian J.* **2012**, *7*, 1426–1434.
- (74) Wu, W.; Zhang, J.; Yang, H.; Jin, B.; Hue, Y.; Hua, J.; Jing, C.; Long, Y.; Tian, H. *J. Mater. Chem.* **2012**, *22*, 5382–5389.
- (75) De Sousa, S.; Ducasse, L.; Kauffmann, B.; Toupance, T.; Olivier, C. *Chem.—Eur. J.* **2014**, *20*, 7017–7024.
- (76) Colombo, A.; Dragonetti, C.; Marinotto, D.; Righetto, S.; Roberto, D.; Tavazzi, S.; Escadeillas, M.; Guerschais, V.; Le Bozec, H.; Boucekkine, A.; Latouche, C. *Organometallics* **2013**, *32*, 3890–3894.
- (77) Boixel, J.; Guerschais, V.; Le Bozec, H.; Jacquemin, D.; Amar, A.; Boucekkine, A.; Colombo, A.; Dragonetti, C.; Marinotto, D.; Roberto, D.; Righetto, S.; De Angelis, R. *J. Am. Chem. Soc.* **2014**, *136*, 5367–5375.
- (78) Frisch, M. J.; Trucks, G. W.; Schlegel, H. B.; Scuseria, G. E.; Robb, M. A.; Cheeseman, J. R.; Scalmani, G.; Barone, V.; Mennucci, B.; Petersson, G. A.; Nakatsuji, A.; Caricato, M.; Li, X.; Hratchian, H. P.; Izmaylov, A. F.; Bloino, J.; Zheng, G.; Sonnenberg, J. L.; Hada, M.; Ehara, M.; Toyota, K.; Fukuda, R.; Hasegawa, J.; Ishida, M.; Nakajima, T.; Honda, Y.; Kitao, O.; Nakai, H.; Vreven, T.; Montgomery, J. A., Jr.; Peralta, J. E.; Ogliaro, F.; Bearpark, M.; Heyd, J.; Brothers, E.; Kudin, K. N.; Staroverov, V. N.; Kobayashi, R.; Normand, J.; Raghavachari, K.; Rendell, A.; Burant, J. C.; Iyengar, S. S.; Tomasi, J.; Cossi, M.; Rega, N.; Millam, J. M.; Klene, M.; Knox, J. E.; Cross, J. B.; Bakken, V.; Adamo, C.; Jaramillo, J.; Gomperts, R.; Stratmann, R. E.; Yazyev, O.; Austin, A. J.; Cammi, R.; Pomelli, C.; Ochterski, J. W.; Martin, R. L.; Morokuma, K.; Zakrzewski, V. G.; Voth, G. A.; Salvador, P.; Dannenberg, J. J.; Dapprich, S.; Daniels, A. D.; Farkas, Ö.; Foresman, J. B.; Ortiz, J. V.; Cioslowski, J.; Fox, D. J. *Gaussian 09*, Revision A.1; Gaussian, Inc.: Wallingford, CT, 2009.

- (79) Becke, A. D. *J. Chem. Phys.* **1993**, *98*, 5648–5652.
- (80) Binkley, J. S.; Pople, J. A.; Hehre, W. J. *J. Am. Chem. Soc.* **1980**, *102*, 939–947.
- (81) Cossi, M.; Barone, V.; Cammi, R.; Tomasi, J. *Chem. Phys. Lett.* **1996**, *255*, 327–335.
- (82) Miertus, S.; Scrocco, E.; Tomasi, J. *Chem. Phys.* **1981**, *55*, 117–169.